International journal of basic and applied research
www.pragatipublication.com
ISSN 2249-3352 (P) 2278-0505 (E)
Cosmos Impact Factor-5.86

Simulation Of Open circuit fault analysis of Multistage Converter fed Hybrid EV system with PMSM Drive

Samudrala Vijender, B.Nagaraju
1, PG Scholar, Department of Electrical and Electronics Engineering
2, Assistant Professor, Department of Electrical and Electronics Engineering
Vaagdevi College Of Engineering, Bollikunta, Warangal (Dt), TS, India.
vijenderv81@gmail.com

Abstract: The performance of Hybrid Electric Vehicles (HEVs), especially in series architecture, is highly dependent on the reliability of electric drive-motor systems. Any failure in power semiconductor devices, such as Insulated-Gate Bipolar Transistors (IGBTs), used in three-phase Voltage Source Inverters (VSIs) for Permanent Magnet Synchronous Motor (PMSM) drive systems, causes a reduction in the reliability and leads to unscheduled maintenance of HEVs. This paper aims to present a three-stage combined model-based and data-driven fault diagnosis approach, the so-called hybrid fault diagnosis approach, to detect, locate, and clear open-circuit faults in IGBTs used in VSI-fed PMSM drive systems in HEVs. Field-Oriented Control (FOC), which is a model-based technique, is used to control the electric drive-motor system. The proposed method, which is based on phase voltage analysis, estimates the current in each phase of VSI using the normal operating conditions dataset to detect open-circuit faults in IGBTs. Once a fault is detected, it is located using the faulty conditions dataset and an online data-driven approach, called the Modified Multi-Class Support Vector Machine (MMC-SVM) algorithm. Thereafter, the faulty IGBT is bypassed by closing the corresponding backup switch, ensuring the continuous operation of the electric drive-motor system. The proposed method can accurately and quickly detect, locate, and clear open-circuit faults in IGBTs without the need for additional sensors. Additionally, it demonstrates robustness against back-to-back and simultaneous faults in IGBTs used in VSI-fed PMSM drive systems in HEVs.

Key Words: Hybrid Electric Vehicles, Insulated-Gate Bipolar Transistors, Voltage Source Inverters, Permanent Magnet Synchronous Motor and MMC-SVM.

I. Introduction

In the past few decades, environmental concerns for fossil fuel-based transportation infrastructure have caused tremendous interest in more electric transportation infrastructure. Unlike Internal Combustion Engine (ICE)-based vehicles that mainly rely on petroleum, a significant portion of consumed power by Hybrid Electric Vehicles (HEVs) is from different energy sources, such as batteries, fuel cells, supercapacitors, etc., along with using electric drive-motor systems [1], [2]. Despite the benefits of HEVs, such as less greenhouse gas emissions, less noise pollution, and higher energy efficiency, failures in their main components, particularly the Permanent Magnet Synchronous Motor (PMSM), Voltage

Source Inverter (VSI), Energy Storage System (ESS), etc., incur heavy expenses and may put the safety of HEVs in danger [3], [4].
Early-stage failures can be due to overvoltage, overcurrent, or overheating in components such as batteries and/or electric drive-motor systems, and it may be more difficult to diagnose failures if other factors, such as noise, vibration, electromagnetic field, frequency, torque, etc., are involved [5], [6]. Hence, to minimize the computational burden and fast recovery of the HEV, it is crucial to find the source of failure. In particular, the major faults of ESSs, specifically batteries, in HEVs can be due to (1) overcharge/ discharge, (2) overheating/undercooling, (3) short circuit/open-circuit of internal cells, and (4) incorrect state estimation [7], [8], [9]. In addition, (1) abnormal connection
of stator windings, (2) short circuit/open-circuit of stator windings, (3) short circuit of rotor windings, (4) broken rotor bars, (5) eccentricity-related faults, and (6) bearing faults are the main faults of electric motors, particularly PMSMs, in HEVs [11], [12]. Moreover, (1) short circuit/open-circuit faults of switches and (2) intermittent gate-misfiring faults are the dominant faults in electric drive systems, mainly VSIs, in HEVs [13], [14].
The risk of failure of power semiconductor devices, particularly Insulated-Gate Bipolar Transistor Bipolar Transistors (IGBTs), used in VSI-fed PMSM drive systems is high. This is due to the fact that such devices are exposed to thermal stress and various harsh environmental and operating conditions. Fault diagnosis of power semiconductor devices has been investigated in many research studies. Short circuit faults in power semiconductor devices occur rapidly and can cause potential destruction. Using hardware protection systems, such faults can be cleared in electric drive systems. A summary of hardware protection systems for short circuit faults is provided in [15]. The impacts of open-circuit faults in power semiconductor devices can potentially lead to VSIs malfunctioning, and consequently their outage and great economic loss [16]. In this regard, various fault-tolerant control approaches are presented in the literature [17], [18], [19], [20], [21] aiming at fast fault diagnosis. Open-circuit fault diagnosis approaches can be either current-based or voltage-based methods. In current-based approaches, (1) there is no need for additional sensors, and (2) by employing the existing current sensors in the control loop, current can be measured to diagnose the fault.

II. Permanent Magnet Synchronous Motors

A three phase PMSM is normally constructed with sinusoidal distributed phase windings, with a 120 phase shift between the three windings. In a stator reference frame coordinate system the phase vectors A;B;C can be seen as they are axed in angle, but with time varying amplitudes. This three vector representation makes calculation of machine parameters unnecessarily complex. By transforming the system into a two vector orthogonal system, the necessary calculations could be much simpler.

a) PMSM design

To be able to simulate the electrical behaviour of the motor in any electrical circuit analysis program the motors equivalent circuit (figure 1) is needed. By transforming the drive voltage into dq parameters and connecting it to its respective dq equivalent circuit, measurement of

International journal of basic and applied research
www.pragatipublication.com
ISSN 2249-3352 (P) 2278-0505 (E)
Cosmos Impact Factor-5.86

the models currents can be done. From the current values the motors torque can be calculated and

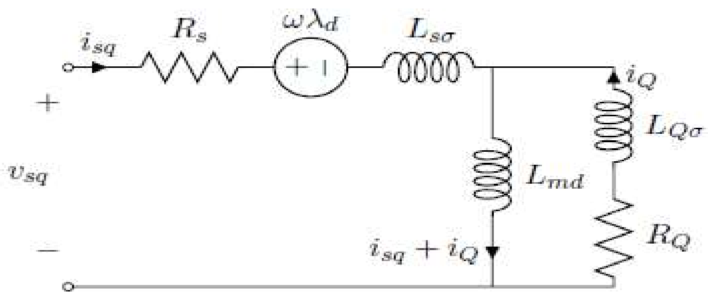

Figure 1 Salient pole machine equivalent circuit

$$\frac{p}{2}(T_e - T_L) = J\frac{d\omega_r}{dt}$$

Where TL is the load torque, !r is the rotational speed and J is the motor and loads inertia. With the above parameters it is possible to implement a model of a PMSM in a circuit simulation software. However, in this thesis the existing Simulink model has been used.

b) Field Oriented Control (FOC)

In Field Oriented Control the goal is to control the direct- and quadratureaxis current id and iq to achieve the requested torque. By controlling id and iq independently it's possible to achieve a Maximum Torque Per Ampere ratio (MPTA) to minimize the current needed for a speci_c torque, which maximizes the motors efficiency.

$$T_{en} = i_{qn}(1 - i_{dn})$$

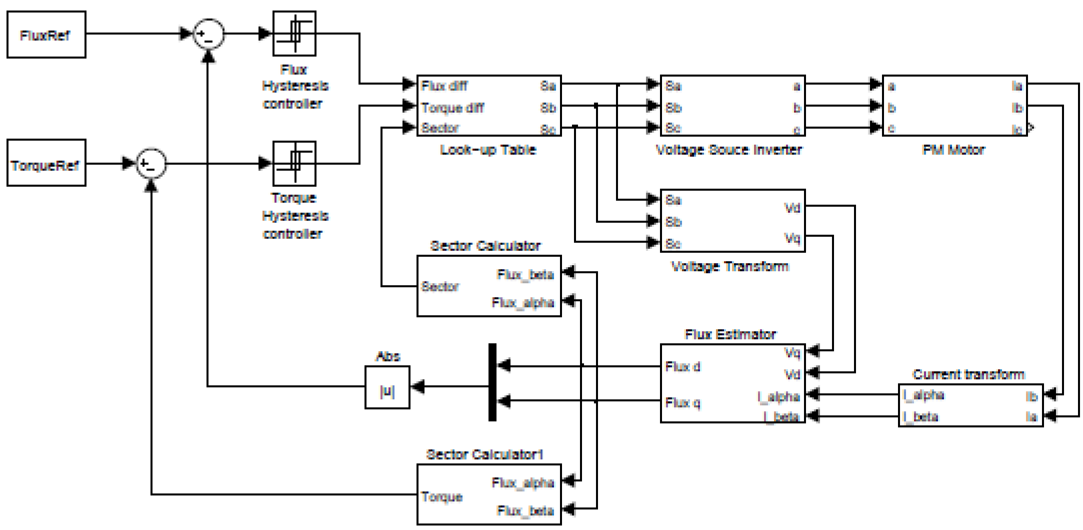

Figure 2 FOC control layout Current Transform

$$i_n = \sqrt{i_{dn}^2 + i_{qn}^2} = 1$$

International journal of basic and applied research
www.pragatipublication.com
ISSN 2249-3352 (P) 2278-0505 (E)
Cosmos Impact Factor-5.86

$$T_{en}^{*} = \sqrt{i_{dn}^{*}\left(i_{dn}^{*} - 1\right)^{3}}$$

$$T_{en}^{*} = \frac{i_{qn}^{*}}{2}\left(1 + \sqrt{1 + 4(i_{qn}^{*})^{2}}\right)$$

c) PMSM Drive System

Figure 6.4 shows the structure of a three-phase VSI-fed PMSM drive system using Field-Oriented Control (FOC). The main role of the control section is to generate the gate pulses based on the expected voltage and feed them into the VSI. The output of the VSI is applied to the PMSM windings to generate continuous current. Each leg of the VSI consists of two IGBTs, and *ith* IGBT is indicated by *SWi*, which comprises*Qi* and*Di*. Each *SW* is controlled by the gate driver, which sends gate pulses to the corresponding IGBTs. Using a three-phase current sensor, the current in each phase, i.e., *ia*, *ib*, and *ic*, can be measured. In addition, θ*e* and ω, which are the rotor electrical angle and the measured angular velocity, respectively, can be determined using position sensor signal processing. In Figure 1, *V*DC represents the DC voltage across the DC-link capacitor.

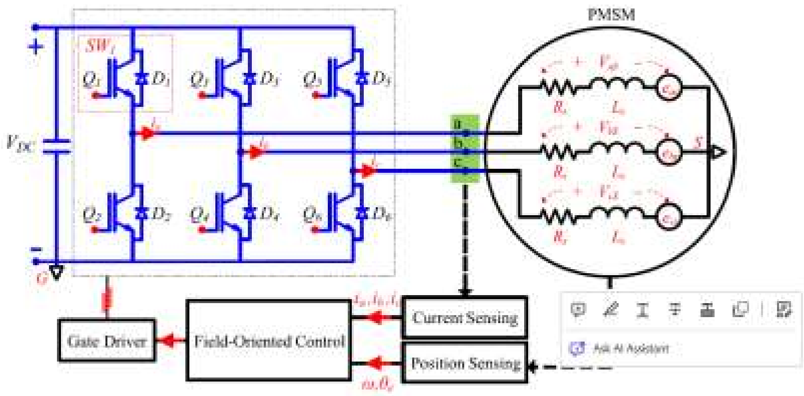

Figure 3 The structure of a three-phase VSI-fed PMSM drive system

d) Phase Voltage Analysis under Normal Operating Conditions

In the VSI-fed PMSM drive system, switching states determine the current flow under different conditions, and accordingly, the output voltage of the VSI varies. Hence, it is necessary to investigate the output voltage under different switching states, and for each *SW*, the switching state can be either ON or OFF. In this case, Table 1 illustrates the relationship between switching states of IGBTs and winding-to-ground voltage of phases *a*, *b*, and *c*, respectively, i.e., *VN aG*, *VN bG*, and *VN cG*, under normal operating conditions. **1.** The relationship between switching states and the winding-to-ground voltage under normal operating conditions.

Table 1 Switching states

Index in Cosmos
2024, Volume 14, ISSUE 4
UGC Approved Journal

State Number	SW_1	SW_2	SW_3	SW_4	SW_5	SW_6	V_{aG}^N	V_{bG}^N	V_{cG}^N
0	OFF	ON	OFF	ON	OFF	ON	0	0	0
1	OFF	ON	OFF	ON	ON	OFF	0	0	V_{DC}
2	OFF	ON	ON	OFF	OFF	ON	0	V_{DC}	0
3	OFF	ON	ON	OFF	ON	OFF	0	V_{DC}	V_{DC}
4	ON	OFF	OFF	ON	OFF	ON	V_{DC}	0	0
5	ON	OFF	OFF	ON	ON	OFF	V_{DC}	0	V_{DC}
6	ON	OFF	ON	OFF	OFF	ON	V_{DC}	V_{DC}	0
7	ON	OFF	ON	OFF	ON	OFF	V_{DC}	V_{DC}	V_{DC}

In a three-phase PMSM with star-connected winding, the following condition is satisfied by Kirchhoff's law:

$$i_a + i_b + i_c = 0$$

In addition, considering the sinusoidal air-gap magnetic flux distribution, the summation of phase voltage is equal to zero.

$$V_{aS} + V_{bS} + V_{cS} = R_s(i_a + i_b + i_c) + L_s\frac{d}{dt}(i_a + i_b + i_c) + (e_{aS} + e_{bS} + e_{cS}) = 0$$

where VaS , VbS , and VcS show the phase voltage of phases *a*, *b*, and *c*, respectively, Rs and Ls are the stator resistance and inductance, respectively, and eaS , ebS , and ecS indicate the corresponding phase back Electromotive Forces (EMFs) of phases *a*, *b*, and *c*, respectively.
Moreover,

$$\begin{cases} V_{aG} = V_{aS} + V_{SG} \\ V_{bG} = V_{bS} + V_{SG} \\ V_{cG} = V_{cS} + V_{SG} \\ V_{SG} = {}^1\!/\!{}_3(V_{aG} + V_{bG} + V_{cG}) \end{cases}$$

e) Phase Voltage Analysis under Faulty Conditions

In a VSI, the switching pulses as well as the direction of the current flow determine its output voltage. Assuming that the current is positive while flowing into the PMSM winding, the switching states, the direction of current in each phase, and accordingly, the voltage of each phase of the VSI can be determined. Figure 2 shows the current paths of phase *a* when an open-circuit fault occurs in $Q1$. In case of an open-circuit fault in $Q1$, indicated by superscript $FSW1$, $SW1$ and $SW2$ are switched OFF. Taking switching state 4 into consideration, if $i1 > 0$, the current of phase *a* flows through $D2$, the relationship between the switching states, the phase voltage, and the current direction in the case of an open-circuit fault in $Q1$ is derived, and the results are shown in Table 1, in which the current direction indicator ϵx (x represent the corresponding phase) can be either ϵa for $ia > 0$ or ϵa for $ia \leq 0$, where $\epsilon a + \epsilon a = 1$. Considering the results of Table 3 and the state of $SW1$ and $SW2$, which are both switched OFF, the phase voltage V

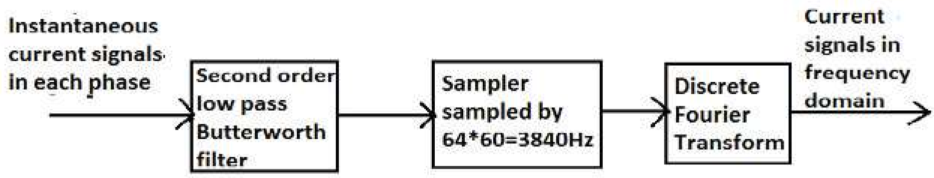

Figure 4 Current controller

III. Simulation Results

A. Normal Operating Conditions

It is assumed that the HEV is accelerating on a straight road between 0.45 and 2.0 s, and during this time period, its velocity increases from 0 to 25.8 km/h. For 0.20 s, the velocity gradually decreases, and at 2.20 s, the brake is applied, which leads to a reduction in the velocity of the HEV to 0 km/h. Figures 5 to 8 show the vehicle speed, PMSM torque, and three-phase current under normal operating conditions, respectively. It is also noted that under normal operating conditions, the DC-link voltage is regulated at 338.14 V.

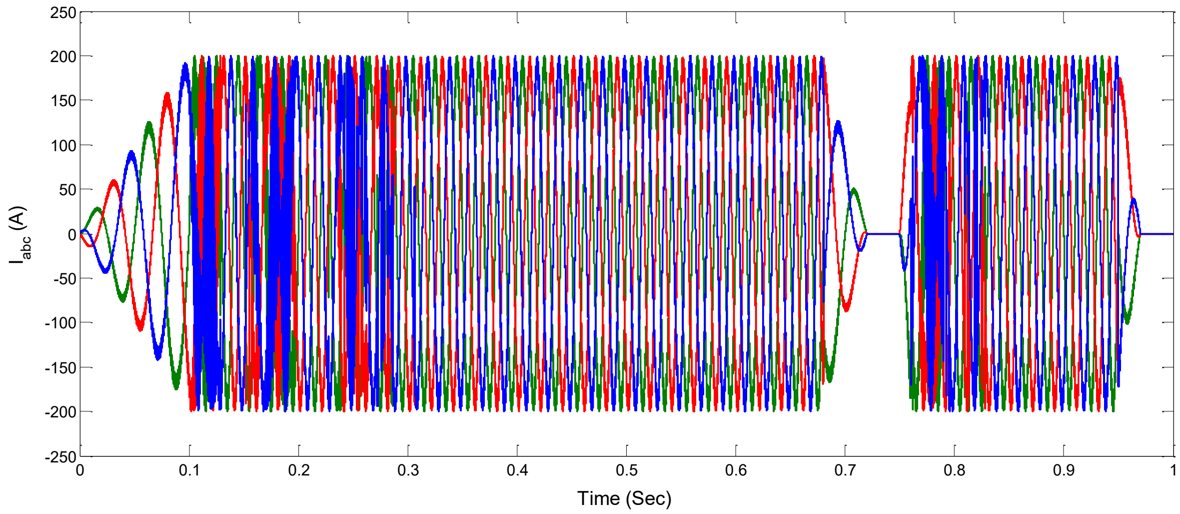

Figure 5 The three-phase current of the PMSM under normal operating conditions.

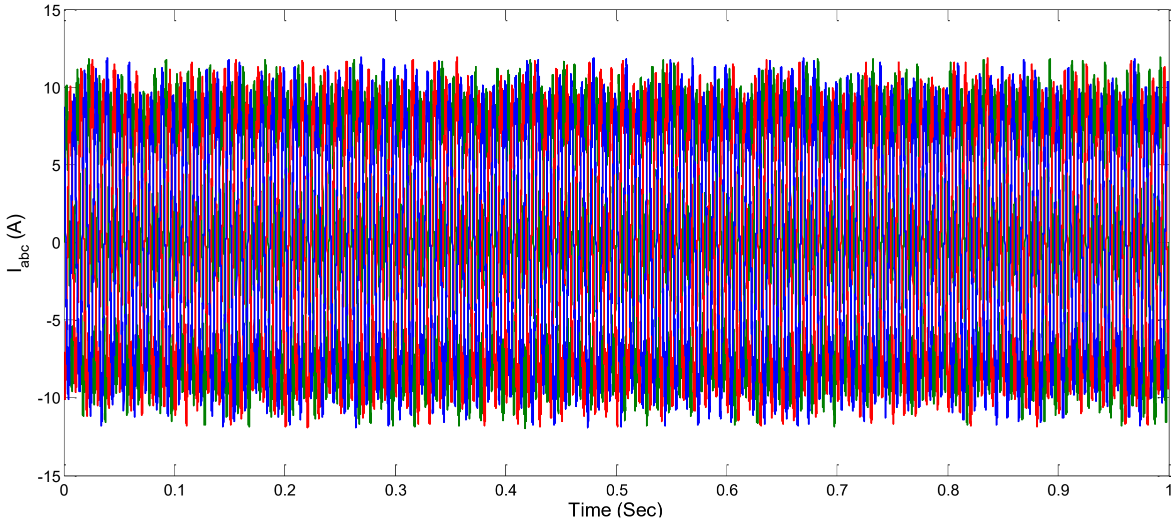

Figure 6 The three-phase residual current of the PMSM under normal operating conditions.

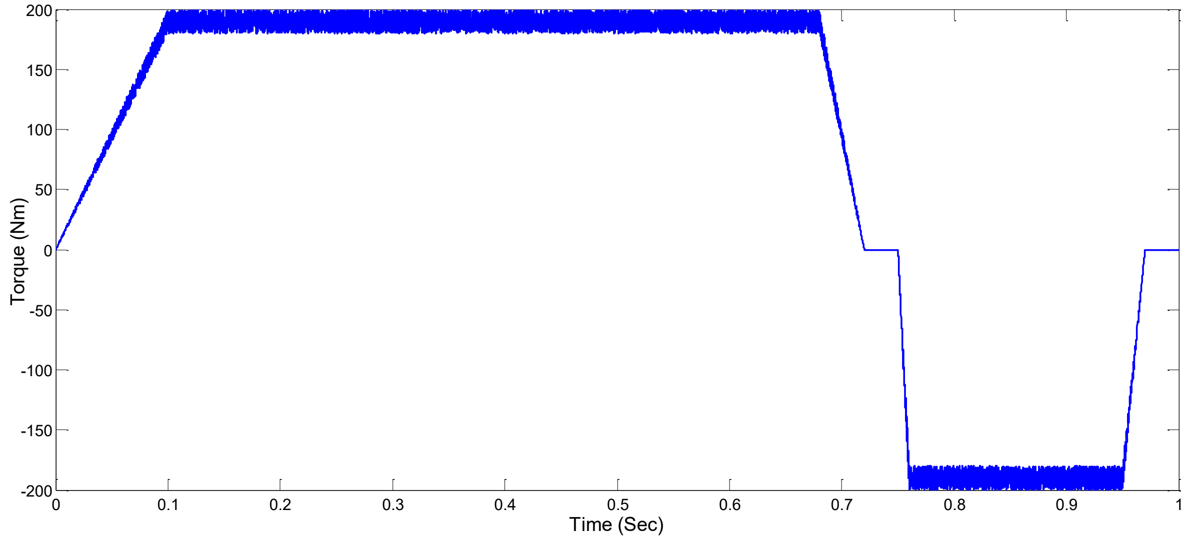

Figure 7 PMSM Torque

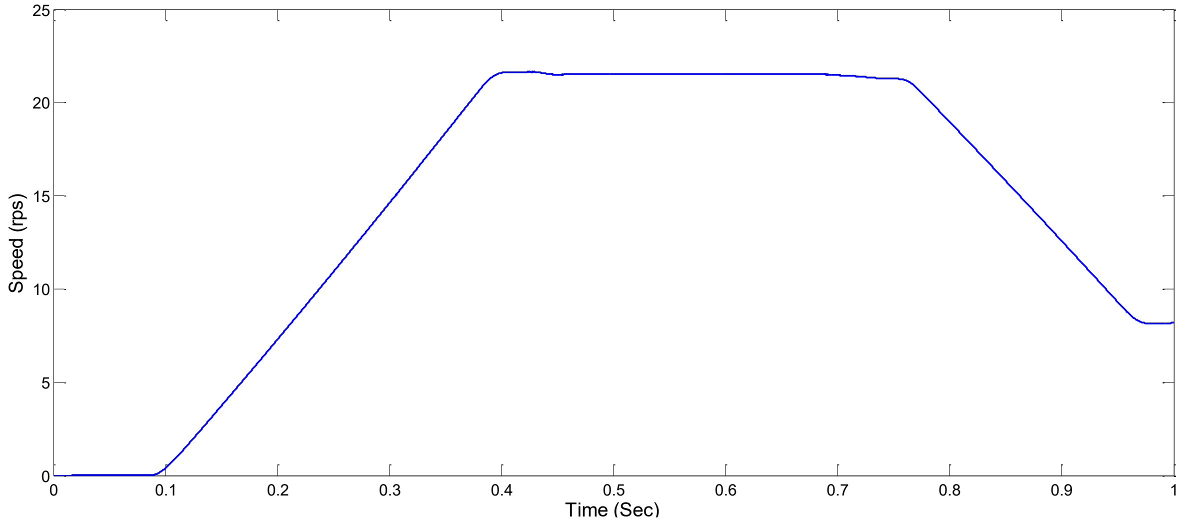

Figure 8 PMSM Speed

B. Open-Circuit Fault in Single Switch

It is assumed that at t = 1 s, an open-circuit fault occurs in the first switch (SW1) and persistently exits till the end of simulation time. Figure 9 shows the three-phase current of the PMSM in case of an open-circuit fault in SW1, in which no current limiter is used to clearly indicate the Rate of Rise (RoR) of the three-phase current. The open-circuit fault in SW1 causes an increase in the current of phases b and c by 8% and 70%, respectively. Changes in the vehicle speed directly cause a significant increase in the current of phases b and c by roughly 8 times, open-circuit fault in SW1.

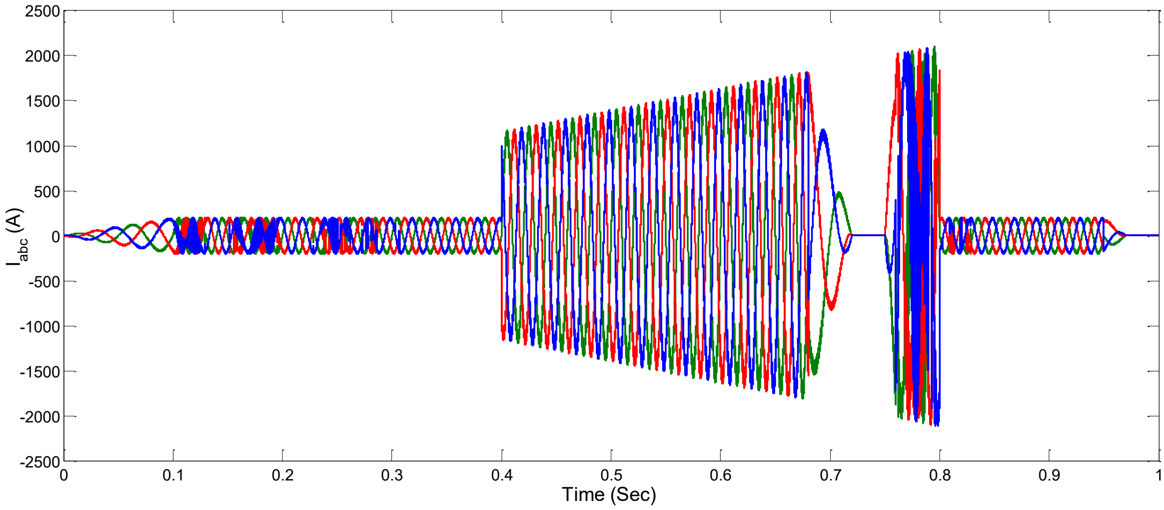

Figure 9 The 3Φ current of the PMSM under fault conditions

International journal of basic and applied research
www.pragatipublication.com
ISSN 2249-3352 (P) 2278-0505 (E)
Cosmos Impact Factor-5.86

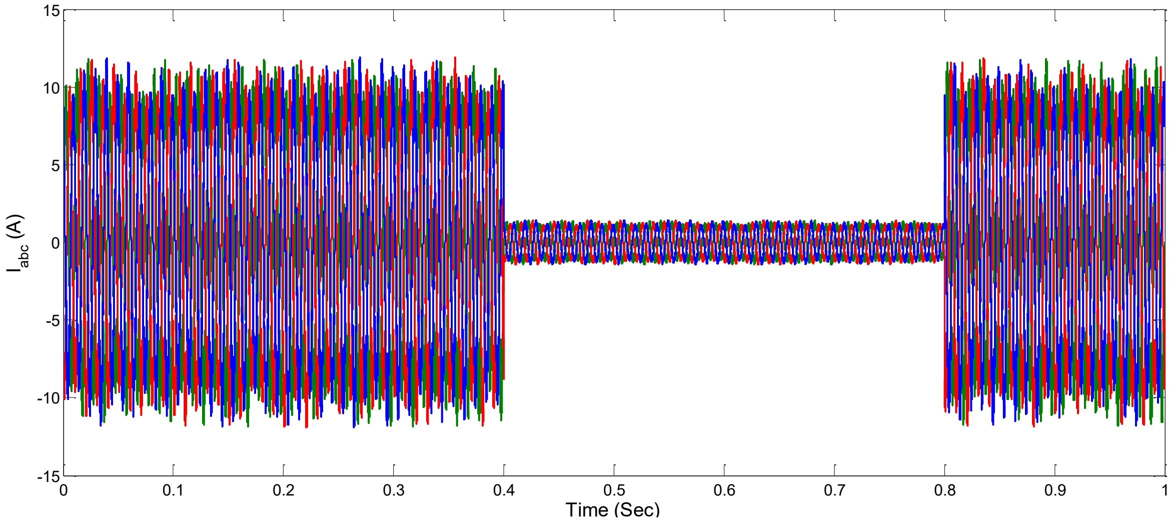

Figure 10 The 3Φ residual current of the PMSM under fault conditions.

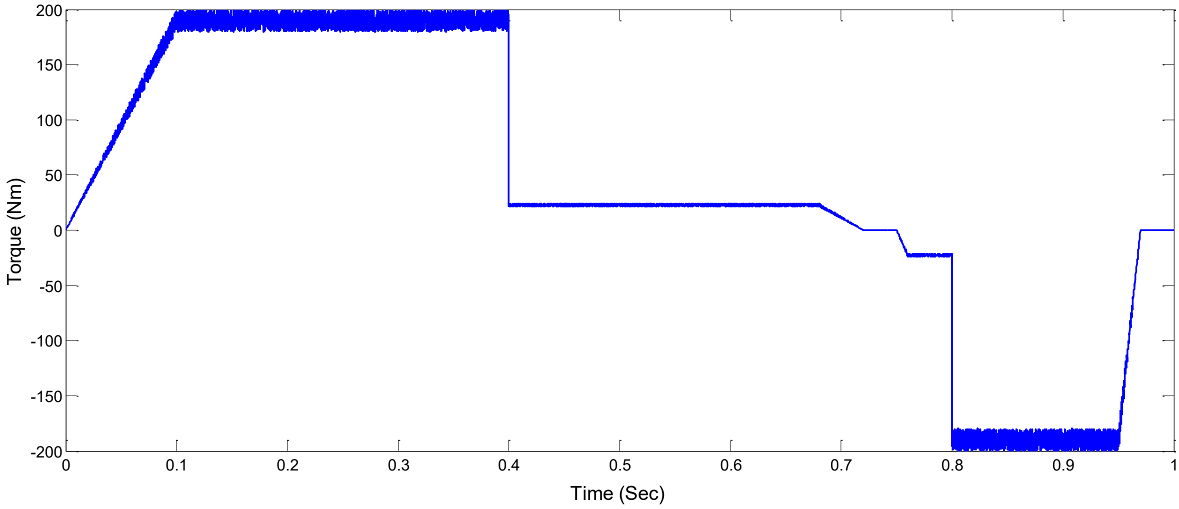

Figure 11 PMSM Torque under fault

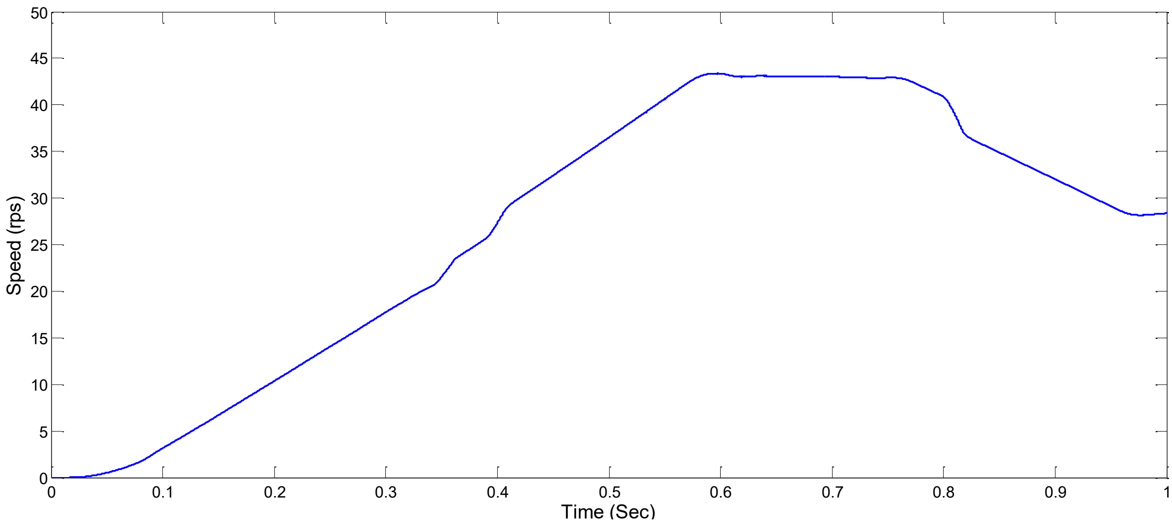

Figure 12 PMSM Speed under fault

Figure 10 demonstrates the three-phase residual current of the PMSM in case of an open-circuit fault in SW1. Since the MMC-SVM algorithm is trained with a set of faulty scenarios. Once the open-circuit fault in SW1 is detected and located, according to Figure 4, the corresponding backup switch. As mentioned earlier, there is a strict time period to clear the fault, i.e., 2 ms, and if the fault is not cleared within the mentioned time period, the VSI-fed PMSM drive system becomes uncontrollable. As an open-circuit fault in SW1 is detected, the fault detection and localization flags maintain their previous conditions, but the VSI-fed PMSM drive system restores to its normal operating conditions. In addition,

VI. Conclusion

In this thesis, a fast online fault diagnosis approach for open-circuit faults in Insulated-Gate Bipolar Transistors (IGBTs) used in Voltage Source Inverter (VSI)-fed Permanent Magnet Synchronous Motor (PMSM) drive systems in Hybrid Electric Vehicles (HEVs) is proposed. The proposed approach incorporates a three-stage combined model-based, data-driven, and fuzzy logic-based fault diagnosis method to efficiently detect, locate, and mitigate open-circuit faults in IGBTs without the need for additional sensors.

In the first stage, the three-phase voltage signals under normal and faulty conditions are analyzed, and the current in each phase is estimated using the normal dataset to detect open-circuit faults. At the second stage, the dataset collected under faulty conditions is analyzed using a Modified Multi-Class Support Vector Machine (MMC-SVM) algorithm with a Radial Basis Function (RBF) kernel function to accurately locate the fault. In the third stage, the method bypasses the fault by sending a closing command to corresponding backup switches, ensuring continuous operation of the VSI-fed PMSM drive system. To further enhance fault detection, a fuzzy logic-based system is integrated into the approach to refine fault classification, improving decision-making accuracy, especially under uncertain or ambiguous conditions.

References

[1] F. Mohammadi, ‘‘Design, analysis, and electrification of a solar-powered electric vehicle,’’ *J. Sol. Energy Res.*, vol. 3, no. 4, pp. 293–299, Dec. 2018.

[2] F. Mohammadi, G.-A. Nazri, and M. Saif, ‘‘A bidirectional power charging control strategy for plug-in hybrid electric vehicles,’’ *Sustainability*, vol. 11, no. 16, p. 4317, Aug. 2019.

[3] C. Mehdipour, F. Mohammadi, and I. Mehdipour, ‘‘Analytical approach to nonlinear behavior study of an electric vehicle,’’ in *Proc. 6th Int. Conf. Control, Instrum. Autom. (ICCIA)*, Oct. 2019, pp. 1–7.

[4] F. Mohammadi, G.-A. Nazri, and M. Saif, ‘‘Modeling, simulation, and analysis of hybrid electric vehicle using MATLAB/simulink,’’ in *Proc. Int. Conf. Power Gener. Syst. Renew. Energy Technol. (PGSRET)*, Aug. 2019, pp. 1–5.

[5] F. Mohammadi and R. Rashidzadeh, ''An overview of IoT-enabled monitoring and control systems for electric vehicles,'' *IEEE Instrum. Meas. Mag.*, vol. 24, no. 3, pp. 91–97, May 2021.
[6] F. Mohammadi and M. Saif, ''A comprehensive overview of electric vehicle batteries market,'' *e-Prime - Adv. Electr. Eng., Electron. Energy*, vol. 3, Mar. 2023, Art. no. 100127.
[7] F. Mohammadi, M. Sanjari, and M. Saif, ''A real-time blockchain-based state estimation system for battery energy storage systems,'' in *Proc. IEEE Kansas Power Energy Conf. (KPEC)*, Apr. 2022, pp. 1–4.
[8] F. Mohammadi, ''Lithium-ion battery state-of-charge estimation based on an improved Coulomb-counting algorithm and uncertainty evaluation,'' *J. Energy Storage*, vol. 48, Apr. 2022, Art. no. 104061.
[9] B. Akin, S. Choi, and H. A. Toliyat, ''DSP applications in electric and hybrid electric vehicles [in the spotlight],'' *IEEE Signal Process. Mag.*, vol. 29, no. 3, pp. 133–136, May 2012.
[10] S. A. Gadsden and S. R. Habibi, ''Model-based fault detection of a battery system in a hybrid electric vehicle,'' in *Proc. IEEE Vehicle Power Propuls. Conf.*, Sep. 2011, pp. 1–6.
[11] M. El Hachemi Benbouzid, ''A review of induction motors signature analysis as a medium for faults detection,'' *IEEE Trans. Ind. Electron.*, vol. 47, no. 5, pp. 984–993, Oct. 2000.
[12] S. Nandi, H. A. Toliyat, and X. Li, ''Condition monitoring and fault diagnosis of electrical motors—A review,'' *IEEE Trans. Energy Convers.*, vol. 20, no. 4, pp. 719–729, Dec. 2005.
[13] K.-T. Chau, ''A software tool for learning the dynamic behavior of power electronics circuits,'' *IEEE Trans. Educ.*, vol. 39, no. 1, pp. 50–55, Feb. 1996.
[14] M. A. Masrur, Z. Chen, and Y. Murphey, ''Intelligent diagnosis of open and short circuit faults in electric drive inverters for real-time applications,'' *IET Power Electron.*, vol. 3, no. 2, p. 279, 2010.
[15] B. Lu and S. K. Sharma, ''A literature review of IGBT fault diagnostic and protection methods for power inverters,'' *IEEE Trans. Ind. Appl.*, vol. 45, no. 5, pp. 1770–1777, Sep. 2009.
[16] J. O. Estima and A. J. M. Cardoso, ''A new algorithm for real-time multiple open-circuit fault diagnosis in voltage-fed PWM motor drives by the reference current errors,'' *IEEE Trans. Ind. Electron.*, vol. 60, no. 8, pp. 3496–3505, Aug. 2013.
[17] U.-M. Choi, F. Blaabjerg, and K.-B. Lee, ''Reliability improvement of a T-type three-level inverter with fault-tolerant control strategy,'' *IEEE Trans. Power Electron.*, vol. 30, no. 5, pp. 2660–2673, May 2015.
[18] U.-M. Choi, J.-S. Lee, F. Blaabjerg, and K.-B. Lee, ''Open-circuit fault diagnosis and fault-tolerant control for a grid-connected NPC inverter,'' *IEEE Trans. Power Electron.*, vol. 31, no. 10, pp. 7234–7247, Oct. 2016.
[19] D. Zhou, Y. Li, J. Zhao, F. Wu, and H. Luo, ''An embedded closed-loop fault-tolerant control scheme for nonredundant VSI-fed induction motor drives,'' *IEEE Trans. Power Electron.*, vol. 32, no. 5, pp. 3731–3740, May 2017.
[20] N. K. Nguyen, F. Meinguet, E. Semail, and X. Kestelyn, ''Fault-tolerant operation of an open-end winding five-phase PMSM drive with short-circuit inverter fault,'' *IEEE Trans. Ind. Electron.*, vol. 63, no. 1, pp. 595–605, Jan. 2016.

[21] R. R. Errabelli and P. Mutschler, ''Fault-tolerant voltage source inverter for permanent magnet drives,'' *IEEE Trans. Power Electron.*, vol. 27, no. 2, pp. 500–508, Feb. 2012.
[22] R. Peuget, S. Courtine, and J.-P. Rognon, ''Fault detection and isolation on a PWM inverter by knowledge-based model,'' *IEEE Trans. Ind. Appl.*, vol. 34, no. 6, pp. 1318–1326, Nov. 1998.
[23] A. M. S. Mendes and A. J. M. Cardoso, ''Voltage source inverter fault diagnosis in variable speed AC drives by the average current Park's vector approach,'' in *Proc. IEEE Int. Electric Mach. Drives Conf. (IEMDC)*, May 1999, pp. 704–706.